Thermal modeling of RF FinFET PAs through temperature-dependent X-parameters extracted from physics-based simulations

Thermal modeling of RF FinFET PAs through temperature-dependent X-parameters extracted from physics-based simulations

E. Catoggio, S. Donati Guerrieri, C. Ramella, F. Bonani
Dipartimento di Elettronica e Telecomunicazioni, Politecnico di Torino
Corso Duca degli Abruzzi, 24, I-10129 Torino, ITALY

***Abstract*—FinFET RF technology is increasingly investigated for the deployment of 5G communication systems and beyond. Thermal management represents one of the main problems that must be addressed for the successful design of FinFET-based microwave power amplifiers. In fact, the peculiar 3D device structure inhibits the efficient heat dissipation through the substrate, requiring an accurate temperature-dependent nonlinear device model. In this paper we extract the FinFET X-parameters from accurate temperature dependent physics-based simulations. The T-dependent X-parameters are then included into Keysight ADS using a dedicated isolated port to represent the device junction temperature. With this modeling approach, we present the T-dependent analysis of a low-power FinFET amplifier at 70 GHz, showing that with T increasing from 300 K to 390 K we have more than 15% P_{sat} loss, 2 dB gain degradation and 10 percentage points efficiency loss.**

***Index Terms*—Microwave amplifiers, X parameters, electrothermal device model**

I. Introduction

FinFETs, originally developed for digital applications, are promising devices for high frequency analog applications due to their high f_{T} and $f_{\max}$, but they call for dedicated technological solutions to reach the power levels required by small-cell applications, typically about few tens of dBm in the 70 GHz – 80 GHz range. Compared to conventional RF technologies, multi-finger multi-fin parallelization and stacking [1], [2] increase parasitics and technological variability. Furthermore, thermal management is a critical issue, since the peculiar 3D device structure inhibits the efficient heat dissipation through the substrate, making accurate nonlinear electro-thermal models of the active device mandatory.

Technology CAD (TCAD) physical simulations are by far the best environment to accurately describe the active device T-dependent material properties and transport parameters. Our in-house TCAD simulator, implementing both the Large-Signal (LS) and Small-Signal Large-Signal (SS-LS) analyses with the Harmonic Balance technique [3], represents a flexible platform to simulate the active device in the operating conditions typical of actual microwave applications, e.g. class B power amplifiers or mixers [4]. Mixed-mode simulations easily couple the active device with the embedding passive structures by either circuit-level or electromagnetic analyses [5]. Physical analysis can also be profitably exploited for the extraction of active device circuit or compact (black-box) models. In previous works [6], we have proven X-parameters (Xpar) [7] to be an effective behavioral model to directly translate physical simulations into EDA tools, retaining the accuracy of TCAD analysis and the link to the fabrication process (e.g. device doping or workfunction). In this work, we extend the Xpar model including an explicit dependence on the device lattice temperature, assumed to be uniform in the device and hence identified with its junction temperature. The T-dependent Xpar model (T-Xpar) is directly included into Keysight ADS using a dedicated port for the junction temperature that allows for the device simulation with varying ambient temperature, but also to couple an external thermal impedance to describe device self-heating in dynamic LS conditions. Therefore, while the Xpar electrical model does not include any thermal memory effect, the T-Xpar model can be regarded as a first step towards the development of a nonlinear dynamic electro-thermal behavioral model [8], [9].

To demonstrate the capability of the proposed modeling approach, we address the design of a FinFET-based class A low-power amplifier (PA) for small-cell applications at 70 GHz. The T-Xpar model accurately predicts the PA mismatch with respect to the "cold" optimum load with increasing temperature and varying back-off condition. It correctly reproduces the reduction of the maximum output power P_{sat} and the variation of the DC power consumption due to the knee voltage thermal walk-out. With T increasing from 300 K to 390 K we observe more than 15% P_{sat} loss, 2 dB gain degradation and up to 10 percentage points efficiency loss.

II. FinFET T-dependent Xpar model

The Xpar model extends the concept of multiport S-parameters to the nonlinear case. The reflected wave b_{pk} at port p and harmonic k resulting from the incident waves a_{ql} can be expressed as:

$$b_{pk}(|a_{11}|,\omega) = X^{\text{F}}_{pk}(|a_{11}|,\omega,T)$$

978-1-6654-7845-8/22/$31.00 ©2022 IEEE

$$+\sum_{q}\sum_{l=1,\dots N} X^{\mathrm{S}}_{pq,kl}(|a_{11}|,\omega,T)P^{k-l}a_{ql}$$

$$+\sum_{q}\sum_{l=1,\dots N} X^{\mathrm{T}}_{pq,kl}(|a_{11}|,\omega,T)P^{k-l}a^{*}_{ql} \qquad (1)$$

where we assume $X^{\mathrm{T}}_{p1,k1} = 0$ and $P = \exp(\mathrm{j}\angle a_{11})$. Functions X^{F}, X^{S} and X^{T}, depending on the input large signal incident wave $|a_{11}|$, fully identify the model: X^{F} relates to the AM-AM/AM-PM curves with a perfectly matched output impedance (typically 50 Ω), while X^{S} and X^{T} are sensitivity terms accounting for the device response to a (small) load mismatch. Sampling the Xpar model over a prescribed input power interval, we generate a look up table model (black box model) suited for circuit level analysis. Here we adopt the proprietary ADS *.xnp* file format and the corresponding Xpar schematic component [**?**]. In-house TCAD simulations implementing the Harmonic Balance LS and SS-LS analyses of the active device are used (see [6] for details) to extract the T-Xpar model, namely X^{F} from the LS working point and X^{S} and X^{T} from the admittance conversion matrix.

In (1), we explicitly assume that the Xpar model parametrically depends on the (constant) device lattice temperature T. In this case the *.xnp* file must also be parametrized in terms of T and the schematic component must reflect this temperature dependency. To demonstrate the procedure, we consider a FinFET active device in bulk Si technology with the cross section shown in Fig. 1. The two gates are considered as a unique gate contact making the FinFET globally a 2-port [10]. To achieve useful power level for RF applications, we analyze a multifinger FinFET unit cell with 10 fingers of 30 fins each and a fin height of 25 nm, yielding a total gate periphery of 15 μm (only the two lateral channels for each fin are considered). First, the FinFET TCAD large-signal analysis has been carried out exploiting our in-house 2D TCAD device simulator with $N = 10$ harmonics and increasing input power from back-off to approximately 2 dB gain compression. The device is terminated on 50 Ω load. At each input power, T-Xpars have been then extracted, with a 50 Ω reference port impedance, at three *extraction temperatures*, i.e. $T = 300$ K, 340 K, 380 K, and collected into a single *.xnp* file. The corresponding Xpar schematic component, see Fig. 1 (bottom), has an extra DC port with null current to select the device operating temperature. ADS interpolates among the available data in the *.xnp* file, allowing simulation with continuously varying T. A certain degree of extrapolation beyond the interval of the extraction temperatures is also allowed by cubic spline interpolation. This procedure is similar to the one used in [6] to make Xpar depend on other physical quantities (e.g. doping), and to the experimental T-dependent Xpar model proposed in [8]. Fig. 2 shows an example of X^{S} and X^{T} obtained from TCAD analysis. The selected parameters account for the mismatch of

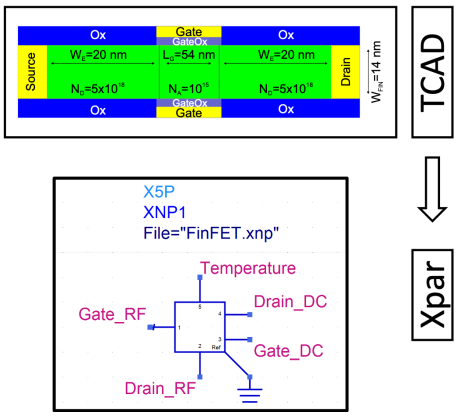

Fig. 1. Top: cross-section of the single fin double gate device used for the TCAD simulations. Bottom: Xpar model used in ADS, showing the extra temperature port.

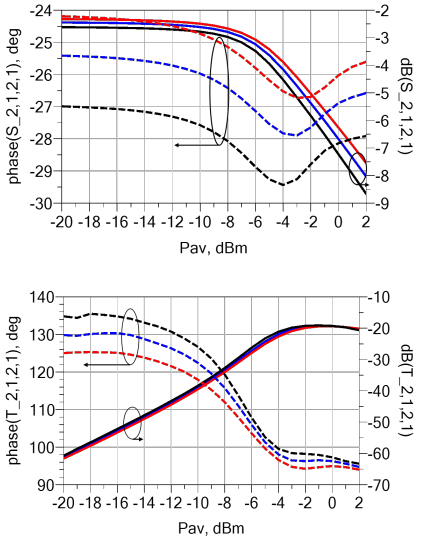

Fig. 2. Temperature dependency of $X^{\mathrm{S}}_{21,21}$ (top) and $X^{\mathrm{T}}_{21,21}$ (bottom) extracted from TCAD analysis. Black: T=300 K; Blue: T=340 K; Red: T=380 K. Solid lines: magnitude. Dashed lines: phase.

the output load with respect to 50 Ω. While $\left|X^{\mathrm{S}}\right|$ shows a significant temperature spread with increasing input power, $\left|X^{\mathrm{T}}\right|$ is nearly constant, consistently with the results in [8]. A non monotonous behavior is observed for the phase, whith up to 10° variation of the X^{T} phase with temperature.

III. FinFET Power Amplifier Analysis

We propose the temperature dependent analysis of a low-power class A amplifier (PA) operating at 70 GHz based on the modelled unit cell [11].

The selected device DC bias is $V_{\mathrm{G}} = 0.675$ V and $V_{\mathrm{D}} = 0.6$ V. The input port is here unmatched and terminated with the same 50 Ω impedance used to extract the Xpars, while the drain port is loaded with the fundamental optimum load $Z_{\mathrm{opt}} = 53 + \mathrm{j}\,6$ Ω and harmonics are shunted by ideal tuners. The PA

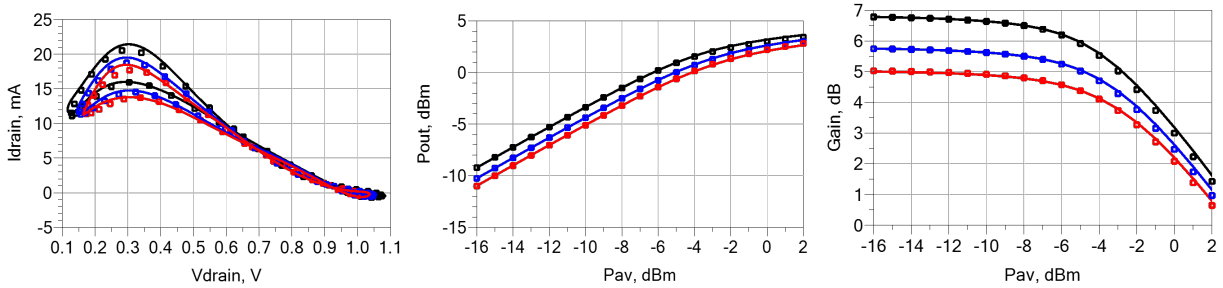

Fig. 3. Left: Dynamic load lines of the FinFET device vs. T, $P_{\mathrm{av}} = 1$ dBm and on optimum load. Center and right: output power and gain vs. T. Solid lines: ADS with X-parameters. Symbols: TCAD physics-based analysis. Black: $T = 300$ K; Blue: $T = 350$ K; Red: $T = 390$ K.

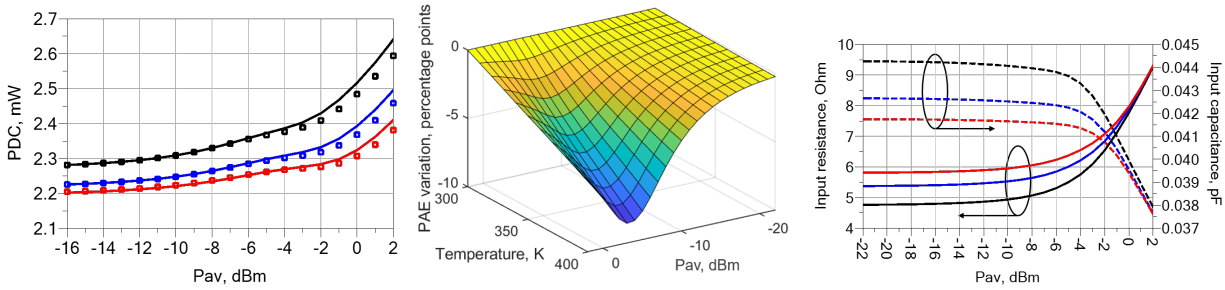

Fig. 4. Left: DC consumption at different temperatures. Center: PAE variation with respect to $T = 300$ K vs. T and input power. Right: Input impedance at different temperatures. Solid lines: ADS with X-parameters. Symbols: TCAD physics-based analysis. Black: $T = 300$ K; Blue: $T = 350$ K; Red: $T = 390$ K.

analysis is carried out with the T-Xpar model in ADS and validated against TCAD simulations for a set of temperatures different from the ones used for the model extraction. Fig. 3 (left) shows the device dynamic load lines (DLLs) on Z_{opt} at $T = 300$ K, 350 K and 390 K. The agreement between TCAD and ADS simulations is always satisfactory, despite the operating condition differs from the model extraction condition both for the load and the temperature. The DLLs show a significant thermal knee walk-out and a global reduction of the overall drain current due to the mobility degradation, hence the optimum load extracted at room temperature will be sub-optimum at higher temperatures. The other plots in Fig. 3 show that both the output power and gain diminish as a function of T. The stage nonlinearity is clearly reflected by the different behavior in back-off and at saturation, with a mild reduction of thermal sensitivity at higher input power. As shown in Fig. 4 (left), the DC power consumption decreases with T, but increases in compression due to the drain current waveform clipping. Combined with the T dependency of P_{out} and gain, the PAE behavior is quite complex. Fig. 4 (center) shows the PAE variation with respect to the "cold" situation: we notice an overall reduction of efficiency with increasing T. Interestingly, the most significant spread occurs around 4 dB to 6 dB of output power back-off, where it is close to 10 percentage points, while in compression it is more limited (around 5 points). Finally, Fig. 4 (right) shows the input impedance: it turns out to strongly depend on T in back-off and less in compression, opening the way to the identification of drive/back-off conditions where the PA input matching is less sensitive to self-heating.

Acknowledgment

This work has been supported by the MIUR PRIN 2017 Project "Empowering GaN-on-SiC and GaN-on-Si technologies for the next challenging millimeter-wave applications (GANAPP)".

References

[1] S. Callender, *et al.*, 2017 IEEE Radio Frequency Integrated Circuits Symposium (RFIC), 4-6 June 2017, Honolulu, HI, USA, DOI: 10.1109/RFIC.2017.7969103

[2] H.-J. Lee *et al.*, *2019 IEEE International Electron Devices Meeting* (IEDM), 7-11 Dec. 2019, San Francisco, CA, USA, DOI: 10.1109/IEDM19573.2019.8993647

[3] S. Donati Guerrieri *et al.*, *IEEE Trans. El. Dev.*, vol. 64, no. 3, p. 1269–1275, DOI: 10.1109/TED.2017.2651168

[4] A.M. Bughio *et al.*, *IEEE El. Dev. Lett.*, vol. 38, no. 8, p. 1004–1007, DOI: 10.1109/LED.2017.2717460

[5] S. Donati Guerrieri *et al.*, *IEEE Journal on Multiscale and Multiphysics Computational Techniques*, vol. 4, no. 1, pp. 356–363, 2019, DOI: 10.1109/JMMCT.2019.2962083

[6] S. Donati Guerrieri *et al.*, 2019 *International Microwave Symposium*, 2–7 June 2019, Boston (MA), USA, DOI 10.1109/mwsym.2019.8700869

[7] D. E. Root *et al.*, *X-parameters*. Cambridge Univ. Press, 2013.

[8] S. J. Gillespie *et al.*, 13th European Microwave Integrated Circuits Conference (EuMIC), 23-25 Sept. 2018, Madrid, Spain, DOI: 10.23919/EuMIC.2018.8539893

[9] F. Bonani *et al.*, *IEEE Microwave Magazine* vol. 9, no. 5, p. 81–89, DOI 10.1109/MMM.2008.927638

[10] A.M. Bughio *et al.*, 11th European Microwave Integrated Circuits Conference (EuMIC), 3-4 Oct. 2016, London, UK, DOI 10.1109/EuMIC.2016.7777534

[11] E. Catoggio *et al.*, *IEEE Trans. El. Dev.*, vol. 68, no. 11, p. 5462–5468, DOI: 10.1109/TED.2021.3076753